Molecular Pharmacology Fast Forward. Published on June 23, 2017 as DOI: 10.1124/mol.117.108712
This article has not been copyedited and formatted. The final version may differ from this version.

MOL #108712

A functional $Na_V1.7$- Na_VAb chimera with a reconstituted high affinity ProTx-II binding site

Ramkumar Rajamani, Sophie Wu, Iyoncy Rodrigo, Mian Gao, Simon Low, Lisa Megson, David Wensel, Rick L. Pieschl, Debra J. Post-Munson, John Watson, David R. Langley, Michael K. Ahlijanian, Linda J. Bristow, and James Herrington

Molecular Discovery Technologies (RR, SW, IR, MG, SL, LM, DW DRL), Wallingford, CT/Princeton, NJ/Waltham, MA, Discovery Biology (RP, DPM, MA, LB, JH) Wallingford, CT and Lead Discovery and Optimization (JW), Bristol-Myers Squibb Company, 5 Research Parkway, Wallingford, CT 06492 USA

Molecular Pharmacology Fast Forward. Published on June 23, 2017 as DOI: 10.1124/mol.117.108712
This article has not been copyedited and formatted. The final version may differ from this version.

MOL #108712

ProTx-II binding to functional $Na_V1.7$-Na_VAb chimera

Address for correspondence:

Ramkumar Rajamani, Ph.D.

Bristol-Myers Squibb

5 Research Parkway

Wallingford, CT 06492

Ramkumar.Rajamani@bms.com

Text Pages : 28

Tables : 0

Figures : 5

References : 51

Abstract (Word Count) : 208

Introduction (Word Count) : 599

Discussion (Word Count) : 1352

Abbreviations:

NaV : Voltage Gated Sodium Channel

CIP : Congenital Insensitivity to Pain

STS : Surrogate Target Strategy

VSD2 : Voltage Sensor Domain 2

SPR : Surface Plasmon Resonance

SPA : Scintillation Proximity Assay

IEM : Inherited Erythromelalgia

PEPD : Paroxysmal Extreme Pain Disorder

CIP : Congenital Insensitivity to Pain

CaV : Voltage-Gated Calcium Channel

Molecular Pharmacology Fast Forward. Published on June 23, 2017 as DOI: 10.1124/mol.117.108712
This article has not been copyedited and formatted. The final version may differ from this version.

Abstract

$Na_V1.7$ is implicated in human pain perception by genetics. Rare gain of function mutations in $Na_V1.7$ lead to spontaneous pain in humans whereas loss of function mutations result in congenital insensitivity to pain (CIP). Hence, agents that specifically modulate the function of $Na_V1.7$ have the potential to yield novel therapeutics to treat pain. The complexity of the channel and the challenges to generate recombinant cell lines with high $Na_V1.7$ expression have led to a surrogate target strategy (STS) approach employing chimeras with the bacterial channel, Na_VAb. In this report we describe the design, synthesis, purification and characterization of a chimera containing part of the voltage sensor domain 2 (VSD2) of $Na_V1.7$. Importantly, this chimera, DII S1-S4, forms functional sodium channels and is potently inhibited by the $Na_V1.7$ VSD2 targeted peptide toxin ProTx-II. Further, we show by [^{125}I]ProTx-II binding and Surface Plasmon Resonance (SPR) that the purified DII S1-S4 protein retains high affinity ProTx-II binding in detergent. We employed the purified DII S1-S4 protein to create a Scintillation Proximity Assay (SPA) suitable for high throughput screening. The creation of a $Na_V1.7$- Na_VAb chimera with the VSD2 toxin binding site provides an important tool for the identification of novel $Na_V1.7$ inhibitors and for structural studies to understand the toxin-channel interaction.

Molecular Pharmacology Fast Forward. Published on June 23, 2017 as DOI: 10.1124/mol.117.108712
This article has not been copyedited and formatted. The final version may differ from this version.

Introduction

The voltage-gated sodium channel $Na_V1.7$, encoded by the gene SCN9A, has a compelling genetic link to human pain perception (Dib-Hajj et al., 2013). Rare mutations in SCN9A which result in over active $Na_V1.7$ channels cause autosomal dominant pain disorders such as inherited erythromelalgia (IEM) and paroxysmal extreme pain disorder (PEPD) (reviewed in (Dib-Hajj et al., 2010). In contrast, rare mutations which result in loss of function of $Na_V1.7$ lead to the recessively inherited congenital insensitivity to pain (CIP) (Cox et al., 2006; Cox et al., 2010; Goldberg et al., 2007). Reduced pain-related behaviors have also been observed in mice with global knock out of $Na_V1.7$ or mice with selective knock out in specific sensory and/or sympathetic neurons (Gingras et al., 2014; Minett et al., 2014; Minett et al., 2012). These results are consistent with an important role for $Na_V1.7$ in pain perception and suggest that selective inhibitors of $Na_V1.7$ may have broad therapeutic potential in a variety of pain conditions.

$Na_V1.7$, like all eukaryotic voltage-gated Na_V channels, is comprised of four domains linked by cytoplasmic loops (Catterall, 2012). Each domain possesses a voltage sensor and pore module. Based on numerous studies over the last 60 years, Na_V channels are expected to have a central pore formed from the S5-S6 segments and four voltage sensing domains (VSD1-VSD4) each comprised of the S1-S4 segments. Structural studies of bacterial Na_V channels (Payandeh et al., 2011; Zhang et al., 2012) and the voltage-gated CaV channel CaV1.1 (Wu et al., 2016; Wu et al., 2015) and the cockroach NavPaS channel (Shen et al., 2017) support this general arrangement. The modular architecture has facilitated pharmacological and structural studies of chimeric channels generated by the transfer of VSDs into related channels. (Ahuja et al., 2015; Alabi et al., 2007; Bosmans et al., 2008; Klint et al., 2015).

Molecular Pharmacology Fast Forward. Published on June 23, 2017 as DOI: 10.1124/mol.117.108712
This article has not been copyedited and formatted. The final version may differ from this version.

The discovery of $Na_V1.7$ inhibitors with sufficient selectivity across the Na_V 1.X family to be effective pain therapeutic agents has proven to be a significant challenge. However, the identification of selective, small molecule aryl sulfonamide $Na_V1.7$ inhibitors targeting the voltage sensor domain 4 (VSD4) have reinvigorated these efforts (Focken et al., 2016; McCormack et al., 2013). Furthermore, landmark structural studies of a chimeric channel where a portion of the VSD4 is grafted onto the bacterial Na_V channel, Na_VAb, has provided key molecular insight into the determinants of selectivity (Ahuja et al., 2015). Despite the considerable promise of selective small molecule inhibitors targeting $Na_V1.7$ VSD4, confirmation of clinical efficacy has not yet been reported for these agents (Cao et al., 2016; Jones et al., 2016).

In addition to VSD4, several other regions of the $Na_V1.7$ channel may be useful for targeting, including the outer pore (Thomas-Tran and Du Bois, 2016; Walker et al., 2012), inner vestibule (Bagneris et al., 2014), and the other VSDs. Notably, VSD2 is the site of interaction of the selective peptide inhibitor ProTx-II (Schmalhofer et al., 2008) and related peptides (Klint et al., 2015; Murray et al., 2015a; Murray et al., 2015b; Murray et al., 2016; Park et al., 2014). Also, this region has been targeted by antibody discovery efforts with some reported success (Lee et al., 2014). We sought to develop a surrogate target strategy (STS) through design of $Na_V1.7$/ Na_VAb chimeric channels incorporating the $Na_V1.7$ ProTx-II binding site into the bacterial channel Na_VAb as a tool for new molecule discovery and structural studies. Here we report the functional characterization of a chimeric protein, referred to as DII S1-S4, and the development of screening assays using this reagent. The DII S1-S4 chimera will be useful in the search for novel $Na_V1.7$ inhibitors targeting this region.

Molecular Pharmacology Fast Forward. Published on June 23, 2017 as DOI: 10.1124/mol.117.108712
This article has not been copyedited and formatted. The final version may differ from this version.

Materials & Methods

Na_VAb chimera construct design. The design focused on replacement of the extracellular loops and significant segment of the transmembrane region of Na_VAb with human DII Na_V1.7 sequence. To identify regions of interest, sequence alignment (ClustalW with default settings) of Na_V1.7 domain II against Na_VAb was performed to identify potential splice junctions within the VSD (Figure 1). For the S1-S2 segment Na_V1.7 (RefSeq NP_002968) the sequence range selected was ILE743-GLU799 covering the E1 loop region and THR810-ARG830 for the SIII-SIV segment covering E2 loop based on conserved residues at the splice junctions. During the course of this effort, reports based on chimeric strategies to generate crystal structures (Ahuja et al., 2015) and identify toxins (Klint et al., 2015) provided support to the viability of this approach.

Expression of Na_VAb chimeras. Recombinant baculovirus (P1) were generated for BirA and all Na_VAb variants using the Bac-to-Bac system (Invitrogen). For large scale expressions, high titer baculovirus (P2) was generated by infecting Sf9 insect cells grown in Hyclone serum free media following the Bac-to-Bac protocol. Sf9 insect cells grown in ESF921 media (Expression Systems) using a Wave Bioreactor System 20/50 EHT (GE Healthcare Life Sciences) was used for recombinant protein expression. Sf9 cells cultured to a density of 2.2 x 10e6 cells/ml were co-infected with the P2 recombinant baculovirus (1-1.5 x 10e8 virus particles/ml) of Na_VAb chimera and BirA at a ratio of 2:1. The infected cells were maintained at 27ºC for 65 hr with bioreactor wave settings suited for 8-10L volumes and the cell pellets were harvested by centrifugation. For expression of non-biotinylated Na_VAb, the same protocol was used except that BirA was omitted.

Protein Purification. The Sf9 cell pellet was resuspended and homogenized in a buffer containing 50 mM Tris (pH 8.0), 250 mM NaCl, benzonase (Sigma Aldrich) and protease inhibitor cocktail (Sigma Aldrich). Cells were then lysed by sonication. Total cell lysate was incubated with 1%

Molecular Pharmacology Fast Forward. Published on June 23, 2017 as DOI: 10.1124/mol.117.108712
This article has not been copyedited and formatted. The final version may differ from this version.

(w/v) n-Dodecyl-β-D-Maltoside (DDM, Anatrace) at 4ºC for one h. Cell debris was removed by centrifugation and the supernatant was collected and incubated with anti-Flag M2 affinity resin (Sigma Aldrich) at 4ºC for overnight for binding. The protein was eluted with a buffer containing 25 mM Tris (pH 8.0), 250 mM NaCl, 0.1% (w/v) DDM and 100 μg mL^{-1} 3x Flag peptide (Sigma Aldrich). The eluted protein was concentrated and loaded onto Superdex-200 columns (GE Healthcare) in DPBS buffer containing 0.1% (w/v) DDM. The peak fraction was collected for all the subsequent work. The majority of the chimera constructs behaved similarly during purification. The level of biotinylation was assessed by LCMS and estimated to be at least 50% of the total.

Cells and reagents. The HEK cell line stably expressing human $Na_V1.7$ (5N/11S splice form) was purchased from Essen Biosciences (Ann Arbor, MI). ProTx-II and Huwentoxin-IV were purchased from Peptides International (Louisville, KY). [^{125}I]ProTx-II was purchased from Perkin Elmer (Waltham, MA). N-terminal 8x His-tagged ProTx-II was a custom synthesis supplied by Smartox Biotechnology (Grenoble, France). Agitoxin-2 was purchased from Alomone Labs (Jerusalem, Israel).

[^{125}I]ProTx-II Binding Assay. ProTx-II binding to Na_VAb chimeras or h $Na_V1.7$ channels was determined with a [^{125}I]ProTx-II binding assay (Schmalhofer et al., 2008). For Na_VAb chimeras, Sf9 cells were collected 54 h after transduction with baculovirus by centrifugation for 20 min at 2000 rpm. The cell pellets were washed once with phosphate-buffered saline (PBS) and stored at -70°C. To prepare purified cell membranes, cell pellets were thawed, suspended in homogenization buffer (50 mM HEPES, 0.1% protease inhibitor cocktail (Sigma catalog# P8340), pH=7.4), and homogenized with 25 strokes of a glass Wheaton tissue grinder on ice. This homogenate was centrifuged at 500 x g for 10 min at 4°C on a Sorvall RC6plus centrifuge. The

Molecular Pharmacology Fast Forward. Published on June 23, 2017 as DOI: 10.1124/mol.117.108712
This article has not been copyedited and formatted. The final version may differ from this version.

supernatant was removed and centrifuged at 38500 x g for 60 min at 4°C. This cell pellet was resuspended in assay buffer (50 mM HEPES, 130 mM NaCl, 5.4 mM KCl, 0.8 mM MgCl, pH=7.4), and protein was determined with a Pierce BCA protein assay kit (Thermo Scientific) with BSA used as protein standard. Binding experiments were performed in a 96 deep-well plate with a reaction volume of 100 µl. Non-specific binding was defined by cold ProTx-II (see figure legends for concentrations). All radioligand incubations were performed at room temperature for 6 h. For DII S1-S4 purified protein binding studies, assay buffer contained 0.05% or 0.25% BSA. The binding reaction was terminated by filtration through GF/B filters for membranes and GF/F filters for purified protein, and filters were washed three times with 2 ml of 4°C wash buffer (DPBS with 10% fetal bovine serum for GF/B filters and 50 mM Tris HCl, pH=7.4, for GF/F filters). Filters were presoaked in 0.5% polyethyleneamine. Bound radioactivity on the filters was counted on a Wallac Wizard gamma counter. Specific [^{125}I]ProTx-II binding values were calculated by subtraction of non-specific binding from total binding for [^{125}I]ProTx-II and expressed as mean counts per min (cpm) ± SEM. IC50 values and saturation binding parameters were calculated from fits using GraphPad Prism 7 as described in the legends. Statistical comparisons were performed using unpaired two-tailed t-tests in Prism.

For whole-cell [^{125}I]ProTx-II binding to h Na$_V$1.7, HEK293 cells stably expressing h Na$_V$1.7 were plated in 96 well poly-D-lysine-coated plates at 15,000 cells per well. After 4 days in culture, media was removed and 100 µl of media containing 0.3 nM [^{125}I]ProTx-II was added. Non-specific binding was determined by the inclusion of 600 nM unlabeled ProTx-II. [^{125}I]ProTx-II was incubated with the cells for 6 h at 37°C. At the end of incubation, radioligand was removed and each well was washed twice with 200 µl of wash buffer (Dulbecco's phosphate-buffer saline, 10% fetal bovine serum). Cells were lysed by addition of 200 µl of 0.2% SDS to each well. The

contents of each well was pipetted into a 5 ml plastic tube and counted on a gamma counter. For [^{125}I]ProTx-II binding to h $Na_V1.7$/HEK293 cell membranes, cells stably expressing h $Na_V1.7$ channels were grown in T-175 flasks. Cells were detached using detachin, pelleted by centrifugation for 10 min at 1000 rpm, and stored at -80°C. h $Na_V1.7$/HEK293 cell membranes were purified as described above for Sf9 membranes.

Patch clamp electrophysiology. Membrane currents were recorded using the whole-cell voltage clamp technique. Data were acquired at 50 kHz via an EPC-10 amplifier with Patchmaster software (HEKA Instruments Inc., Bellmore, NY). Glass microelectrodes had resistances of 1-4 MOhms when filled with intracellular solution. Series resistance was kept below 10 MOhms and compensated at least 50%. Leakage subtraction was performed with the P/N method. Methods for recording wild-type Na_VAb and chimera channel currents in Sf9 cells were adapted from those described by Gamel El-Din et al. (Gamal El-Din et al., 2013). Briefly, Sf9 cells transduced with baculovirus were cryopreserved 24-31 h post-transduction. On the day of recording, cells were rapidly thawed and plated in Sf-900 II SFM (Thermo Fisher). Recordings were performed between 0.5 h and 5 h after plating. The intracellular solution contained (in mM): 105 CsF, 35 NaCl, 10 EGTA, 10 HEPES, pH 7.4 with CsOH. The external solution was (in mM): 140 NaCl, 2 $MgCl_2$, 2 $CaCl_2$, 10 HEPES, pH 7.4 with NaOH. The holding potential was -180 mV. ProTx-II was diluted into external solution supplemented with 0.1% BSA (w:v) and applied to cells by a gravity fed bath perfusion system. For recording $Na_V1.7$ currents in HEK293 cells, the intracellular solution contained (in mM): 50 CsCl, 90 CsF, 10 NaF, 2 $MgCl_2$, 10 EGTA, 10 HEPES, pH 7.2 with CsOH. The external solution was (in mM): 150 NaCl, 4 KCl, 1 $MgCl_2$, 1.8 $CaCl_2$, 10 HEPES, 10 glucose, pH 7.4 with NaOH. The holding potential was -110 mV.

Molecular Pharmacology Fast Forward. Published on June 23, 2017 as DOI: 10.1124/mol.117.108712
This article has not been copyedited and formatted. The final version may differ from this version.

Peak membrane currents and tail current amplitudes were measured with Patchmaster software. Conductance was estimated by dividing the peak current at the test potential by the driving force for sodium. For the DII S1-S4 chimera, conductance was estimated by the tail current amplitude upon repolarization from the test potential. The voltage-dependence of activation was determined by fits of the Boltzmann equation of the form: $G(V) = G_{max} * (1 / (1 + \exp(-(V - V_{1/2}) / k)))$, where G_{max} is the maximal conductance, $V_{1/2}$ is the voltage of half-maximal activation and k is the slope. Fitting and plotting of data were performed with IGOR Pro 6 software (WaveMetrics, Inc., Lake Oswego, OR). Data are presented as mean ± SEM.

Surface Plasmon Resonance (SPR) Assay. Neutravidin (Pierce/Thermo) was amine-coupled to a Biacore T200 CM5 chip (GE Healthcare) via a standard EDC/NHS kit (GE Healthcare) using these parameters: 40 μg/mL Neutravidin in 10 mM sodium acetate, pH 4.5; 37°C; 15 min contact time at 10 μL/min flow rate. These conditions resulted in the coupling of approximately 22,000 response units (RU) of Neutravidin to the chip surface. Neutravidin coupled surfaces were conditioned with three pulses (30 s) of 1 M NaCl, 40 mM NaOH. Biotinylated Na_VAb and chimeras were diluted to 100 nM in PBS with 0.1% w/v n-dodecyl-β -D-maltopyranoside (DDM; Anatrace) and flowed over the Neutravidin surfaces at 25°C on separate flow cells until saturation (typically 1000 to 1200 RU). PBS + 0.1% DDM was used for all subsequent sample dilutions and running buffer at a flow rate of 20 uL/min. Kinetic and steady-state affinity analysis of the resulting binding data was conducted with Biacore T200 Evaluation Software, version 2.0 (GE Healthcare).

[^{125}I]ProTx-II Scintillation Proximity Assay (SPA). Scintillation proximity assays were performed in non-treated white 1536-well assay plates (Corning Life Sciences, Corning, NY). Briefly, 1.5 μL of assay buffer (130 mM NaCl, 5.4 mM KCl, 5 mM glucose, 0.8 mM $MgCl_2$,

0.05% BSA, 0.1% DDM) was dispensed to the assay plate, followed by an equal volume of biotinylated DII S1-S4 protein (3.33 µg/mL). Streptavidin-coated polystyrene imaging beads (1.7 mg/mL; PerkinElmer) were then added, followed by 1.5 µL of radioligand (3.2 nM). Nonspecific binding was determined in the presence of 2 µM unlabeled ProTx-II. The final SPA reaction (6 µL) contained 5 ng DII S1-S4 protein, 2.5 µg/well SPA imaging beads, and 0.8 nM [^{125}I]ProTx-II. DMSO was included in the assay wells at a final concentration of 0.5%. For competition binding experiments, unlabeled ProTx-II was diluted to 4X the final concentration in assay buffer. The sample was diluted 1:3 in assay buffer in a 384-well polypropylene plate (Brooks Automation, Chelmsford, MA) to produce a 16-point dilution series. The final concentration of ProTx-II in the assay ranged from 2500 nM to 0.0017 nM. Unlabeled peptide was preincubated with DII S1-S4 protein for 30 min prior to the addition of SPA beads and radioligand. Following addition of SPA beads and radioligand, the plates were sealed with clear adhesive seals (PerkinElmer) and well luminescence was imaged immediately using a LEADseeker (Amersham, Pittsburgh, PA; instrument settings: 300 s exposure, 2x2 binning). Plates were then incubated at room temperature and imaged at one hour intervals for 12 h. Assay quality and robustness were estimated by calculating the Z' statistic (Zhang et al., 1999) using the total binding wells (high signal) and nonspecific binding wells (low signal). Raw luminescence data were analyzed by nonlinear regression (4-parameter fit) using GraphPad Prism 7 (La Jolla, CA).

Molecular Pharmacology Fast Forward. Published on June 23, 2017 as DOI: 10.1124/mol.117.108712
This article has not been copyedited and formatted. The final version may differ from this version.

Results

Design, expression and characterization of Na$_V$1.7- Na$_V$Ab chimeras. We aimed to design a Na$_V$1.7- Na$_V$Ab chimeric protein that captured key elements of the Na$_V$1.7 DII VSD (Figure 1). Based on sequence alignment we selected a portion of the transmembrane segments including the extracellular loops to represent the target of interest (Na$_V$1.7 DII VSD). The intracellular loops and the remaining segments of the transmembrane region of the template (Na$_V$Ab) were retained. Chimeric proteins were expressed in Sf9 cells using baculovirus techniques. Two independent constructs were generated (DII S1-S4 and DII S3-S4) for functional characterization and evaluation of suitability as a screening reagent (Supplemental Figure 1).

Electrophysiology of DII chimeras. We explored whether the DII chimeras form functional channels when expressed in Sf9 cells. First, we confirmed that Sf9 cells expressing wild-type Na$_V$Ab displayed robust inactivating inward currents characteristic of Na$_V$Ab (Gamal El-Din et al., 2013; Payandeh et al., 2012) while no such currents were detectable in non-transduced Sf9 cells (Supplemental Figure 2). Sf9 cells expressing DII S1-S4 chimera generated currents with distinct characteristics. In response to depolarizations above +50 mV, non-inactivating outward currents were observed and upon repolarization to -180 mV large inward tail currents (Fig. 2A) were seen in 24 out of 39 cells. This current signature is consistent with a voltage-gated channel activating at positive membrane potentials. Tail current analysis estimated a reversal potential close to E_{Na} (+37 mV, see Methods), consistent with a Na conductance. The voltage-dependence of activation of DII S1-S4 channels estimated from tail current analysis suggested that activation is insignificant below 0 mV with a $V_{1/2}$ of +52 mV (Fig. 2B). This activation range is much more positive that wild-type Na$_V$Ab and wild-type h Na$_V$1.7 (Fig. 2B, Supplemental Table 1). In contrast, DII S3-S4 chimera transduced Sf9 cells generated large, inactivating inward currents

Molecular Pharmacology Fast Forward. Published on June 23, 2017 as DOI: 10.1124/mol.117.108712
This article has not been copyedited and formatted. The final version may differ from this version.

similar in appearance to Na_VAb with a $V_{1/2}$ of activation of -38 mV (Supplemental Figure 3; Supplemental Table 1).

Next, DII S1-S4 chimera currents were tested for their sensitivity to ProTx-II. When measured at the test potential of +60 mV, 10 nM ProTx-II inhibited DII S1-S4 tail current by 94 ± 2% (n=3). Inhibition was characterized by a positive shift in the voltage-dependence of activation (Fig. 2D). To quantify the effect of ProTx-II on DII S1-S4 activation we chose a concentration of 100 nM, to avoid long incubation times because of the relative instability of these recordings. At 100 nM, ProTx-II shifted activation by +54 mV and decreased maximal conductance by 24% (Supplemental Figure 4). Hence, ProTx-II is a potent inhibitor of DII S1-S4 channels and acts as a gating modifier, similar to the action of ProTx-II on $Na_V1.7$. In contrast, DII S3-S4 channels were not significantly inhibited by 100 nM ProTx-II (5 ± 11% n=6; data not shown).

Purification of $Na_V1.7$- Na_VAb chimeras. Once expression and function were confirmed, large scale cell cultures (8-10 L) were transduced to yield cell pellets for membrane isolation and protein purification. Wild type Na_VAb and chimeras were purified on anti-Flag M2 affinity columns and eluted protein was solubilized in detergent (0.1% (w/v) DDM). SDS-PAGE analysis demonstrated proteins with the predicted molecular mass (22 kDa, Supplemental Figure 5). Protein purity was estimated to be greater than 90%.

[^{125}I]ProTx-II binding. Radiolabeled ProTx-II binding was also used to test for ProTx-II sensitivity of DII chimeras. A baseline was established with ProTx-II binding to human $Na_V1.7$. As expected, HEK293 cells stably expressing wild-type human $Na_V1.7$ channels displayed robust specific binding of [^{125}I]ProTx-II (Fig. 3A). In membrane preparations from these same cells, no specific binding of [^{125}I]ProTx-II was detectable. The average specific binding window in cells was 5.6-fold compared to 1.1-fold in membranes ($p<0.05$). In membrane preparations from Sf9

Molecular Pharmacology Fast Forward. Published on June 23, 2017 as DOI: 10.1124/mol.117.108712
This article has not been copyedited and formatted. The final version may differ from this version.

cells expressing the DII S1-S4 chimera, significant specific binding of [^{125}I]ProTx-II was apparent (Fig. 3B). Interestingly, non-transduced Sf9 cells displayed a lower but measurable total [^{125}I]ProTx-II binding which was similar to that observed in cells expressing either wild-type Na_VAb or the DII S3-S4 chimera (Fig. 3B). In all cases this binding was largely displaced by cold ProTx-II, suggesting potential alternate site(s) of specific interaction on the Sf9 membrane. Nevertheless, the highest specific [^{125}I]ProTx-II binding was observed in Sf9 membranes expressing the DII S1-S4 chimera (7.2-fold compared to about 4-fold for Sf9, NavAb, or DII S3-S4; $p<0.05$), suggesting direct binding to the DII S1-S4 chimeric protein. Given this observation, we purified DII S1-S4 protein and tested for [^{125}I]ProTx-II binding. Specific [^{125}I]ProTx-II binding was observed with purified DII S1-S4 protein in detergent with a clear dependence on the amount of chimeric protein (Fig. 3C). The highest specific binding was observed at 0.3 μg protein (8.8-fold, $p<0.05$ compared to the other protein concentrations). No specific [^{125}I]ProTx-II binding was detectable with purified DII S3-S4 protein (Supplemental Figure 6).

The [^{125}I]ProTx-II binding data with Sf9 membranes and purified proteins suggested that the DII S1-S4 chimera but not the DII S3-S4 chimera reconstituted the high affinity ProTx-II binding site. To characterize this binding further, we performed competition binding experiments on purified DII S1-S4 protein with cold ProTx-II and a related peptide, Huwentoxin-IV (Fig. 3D). Cold ProTx-II displaced specific [^{125}I]ProTx-II binding with an IC_{50} of 36 nM whereas Huwentoxin-IV was weaker (IC_{50} of 662 nM) consistent with literature (Xiao et al., 2010). Saturation binding experiments of [^{125}I]ProTx-II binding to the DII S1-S4 chimera estimated a Kd of 9.4 nM (Supplemental Figure 7).

SPR Characterization. In order to explore the kinetics of binding interactions between the toxins and DII chimeras, biotinylated versions of the purified Na_VAb, DII S3-S4, and DII S1-S4 proteins

Molecular Pharmacology Fast Forward. Published on June 23, 2017 as DOI: 10.1124/mol.117.108712
This article has not been copyedited and formatted. The final version may differ from this version.

were captured onto a Biacore CM5 chip derivatized with Neutravidin. His-tagged ProTx-II, Huwentoxin-IV, and Agitoxin-2 were then flowed over these surfaces in order to detect binding interactions. As shown in Figure 4, ProTx-II and Huwentoxin-IV bound specifically to the DII S1-S4 chimera, but not to Na_VAb or DII S3-S4 chimera. Agitoxin-2 did not bind to any of these surfaces, as expected (data not shown). In order to test the reproducibility of this system, concentration series of the ProTx-II and Huwentoxin-IV were flowed over these surfaces in duplicate. As shown in Figure 4C and Figure 4D, concentration-dependent binding was detected for both toxins, and sample duplicates demonstrated good reproducibility of the binding signal. These binding data did not fit well to a 1:1 binding model, so on- and off-rates could not be accurately determined. Fitting with a steady-state binding model yielded apparent affinities of 15 nM for ProTx-II and 125 nM for Huwentoxin-IV consistent with the rank order reported in literature for WT human $Na_V1.7$ (Xiao et al., 2010).

SPA Assay. Given the robust binding of ProTx-II to purified DII S1-S4 protein detected by filter binding and SPR, we next sought to develop a Scintillation Proximity Assay (SPA) for screening. Biotinylated DII S1-S4 protein was immobilized on streptavidin-coated SPA beads and incubated with [^{125}I]ProTx-II. Initial studies were performed in 384-well format and subsequently the assay was optimized for 1536-well plates. Optimization for protein and [^{125}I]ProTx-II usage yielded an assay with suitable sensitivity to competition by cold ProTx-II (IC_{50} = 107 nM; Fig. 5A). The IC_{50} of competition by cold ProTx-II peptide was stable for at least 8 h (average IC_{50}: 118 ± 12 nM; range: 99 nM to 135 nM) (Fig. 5B). The reduced potency of ProTx-II in this assay compared to filter binding was likely due to ligand depletion in the low volume format (6 µL). The signal-to-background ratio increased slightly over the first hour of incubation, was then stable for 10 h at room temperature (average: 7.0 ± 0.43) and deceased to the approximate t = 0 level by 12 h (Fig.

Molecular Pharmacology Fast Forward. Published on June 23, 2017 as DOI: 10.1124/mol.117.108712
This article has not been copyedited and formatted. The final version may differ from this version.

5C). Assay robustness, as indicated by the Z' statistic, was stable over the course of the experiment (average Z': 0.62 ± 0.03). As expected, the assay signal was also sensitive to Huwentoxin IV with reduced potency (IC_{50} = 1.3 μM) compared to ProTx-II (data not shown).

Discussion

$Na_V1.7$ is a target of high importance for the development of novel analgesics based on human genetics linking this channel to pain perception. Two sites on $Na_V1.7$ are known to yield selective inhibitors of channel function. Small molecule sulfonamides bind to VSD4, and lock the VSD in the activated conformation, leading to channel inactivation (Ahuja et al., 2015; McCormack et al., 2013). The other site is on VSD2, where gating modifier peptides such as ProTx-II bind (Schmalhofer et al., 2008). ProTx-II inhibits Na_V channels by a distinctly different mechanism - it traps the voltage sensor in the resting state, making it more difficult for voltage to open the channel (Sokolov et al., 2008). While both sites are of significant interest, it is not yet known if these mechanistically distinct approaches to channel inhibition provide any advantage from a therapeutic standpoint. Nevertheless, efforts to thoroughly explore each of these pharmacophores have been rigorous. Here we describe the characterization of a novel chimeric protein comprising the human $Na_V1.7$ DII S1-S4 region with the bacterial Na_V channel, Na_VAb, which is suitable for high throughput screening for novel agents targeting the VSD2 site.

We find the DII S3-S4 and DII S1-S4 chimera's form functional channels with unique properties. Most notably, in comparison to Na_VAb a positive shift in activation of 55 mV for DII S3-S4 and 145 mV for DII S1-S4 respectively. While the DII S3-S4 represents an activation profile closer to that observed for WT-Na_VAb the DII S1-S4 profile renders it such that channel opening is negligible at 0 mV. This activation profile uniquely qualifies the DII S1-S4 for use in identification of modulators that target primarily target the resting state of the channel. We

Molecular Pharmacology Fast Forward. Published on June 23, 2017 as DOI: 10.1124/mol.117.108712
This article has not been copyedited and formatted. The final version may differ from this version.

speculate the large shift in activation profiles originate from changes in the pairing environment of the gating charges spanning the S4 segment of the DII VSD's and can vary dependent on the template used. A right shift in the activation potential for the DII Kv2.1-rat $Na_V1.2$ chimera compared to the template reference (Kv2.1) was also observed in previously reported studies (Bosmans et al., 2008).

Previous studies have found that transferring a section of the helix-turn-helix motif covering E3 loop of $Na_V1.7$ DII S3-S4 to Kv2.1 conferred ProTx-II sensitivity to the channel chimera (Bosmans et al., 2008). Additionally, mutation of individual residues in the DII S3-S4 region (e.g. F813 and E818) reduce ProTx-II sensitivity (Schmalhofer et al., 2008; Xiao et al., 2010). Likewise, a residue (L833) in DII S3 of $Na_V1.2$ is important for ProTx-II inhibition (Sokolov et al., 2008). In contrast, mutation of residues in DII S1-S2 of $Na_V1.5$ did not significantly affect ProTx-II inhibition (Smith et al., 2007). We find that transfer of $Na_V1.7$ DII S3-S4 helix-turn-helix motif to Na_VAb did not yield channels sensitive to ProTx-II. One possible reason for the difference in observation could have been a result of the variation in the inserted sequence. To reconstitute high affinity ProTx-II binding, the helix-turn-helix motif of $Na_V1.7$ DII S1-S2 was also required. These results suggest that in the context of Na_VAb template additional residues of $Na_V1.7$ DII S1-S2 are likely important for ProTx-II binding.

Gating modifier peptides stabilize the resting conformation and affinity is reduced when the voltage sensor is in the activated conformation (Tilley et al., 2014). Hence, the positive activation profile may have allowed for detection of high affinity ProTx-II binding in membranes and with purified protein. Despite the high affinity binding observed with the purified DII S1-S4 chimera (K_d = 30 nM), the binding is weaker than that observed with wild-type human $Na_V1.7$ expressed in HEK293 cells (K_d = 0.3 nM) (Schmalhofer et al., 2008). The lower binding affinity

Molecular Pharmacology Fast Forward. Published on June 23, 2017 as DOI: 10.1124/mol.117.108712
This article has not been copyedited and formatted. The final version may differ from this version.

observed with DII S1-S4 may result from a combination of alternate VSD conformations and/or the influence of the detergent resulting in significantly different environment compared to live HEK293 cells expressing wild-type $Na_V1.7$ (Marheineke et al., 1998). Gating modifier peptides are known to partially partition into membranes (Lee and MacKinnon, 2004; Mihailescu et al., 2014; Milescu et al., 2007) and ProTx-II clearly interacts with phospholipids (Henriques et al., 2016; Smith et al., 2005). Conversely, VSD interactions with lipid can influence toxin binding (Milescu et al., 2009). Auxiliary subunits are also known to influence gating modifier action on Na_V channels (Wilson et al., 2011). Thus, the affinity of DII S1-S4 for ProTx-II is likely impacted by the expression/reconstitution system employed here. Alternatively, other residues present in $Na_V1.7$ VSD2 but not included in the DII S1-S4 chimera may be important for ProTx-II binding either through direct interaction or providing key structural features of the VSD. If so, further refinements of the DII S1-S4 chimera may improve ProTx-II binding affinity. Also, it is important to note that the other VSDs of $Na_V1.7$ appear to interact with ProTx-II (Bosmans et al., 2008; Xiao et al., 2014; Xiao et al., 2010) which would not be captured in the chimera reported here.

Purified DII S1-S4 protein in detergent capable of high affinity ProTx-II binding opens several possibilities for use in discovery efforts. For example, the protein may be useful as an antigen in monoclonal antibody discovery, screening reagent to identify molecules such as toxins, adnectins, synthetic peptides, milla molecules and small molecules. Screening approaches based on detection of binding to the chimera (and not wild-type Na_VAb) may yield molecules that interact specifically with the transplanted residues of DII S1-S4. Furthermore, traditional screening approaches based on competition of [^{125}I]ProTx-II binding are feasible. The ability of purified DII S1-S4 to bind ProTx-II affords several opportunities for assay development not possible with crude membrane preparations containing channels at relatively low density. For example, we were able

Molecular Pharmacology Fast Forward. Published on June 23, 2017 as DOI: 10.1124/mol.117.108712
This article has not been copyedited and formatted. The final version may differ from this version.

convert and miniaturize the [^{125}I]ProTx-II binding assay to a SPA format in 1536 wells. The homogenous assay is sufficiently robust to support high throughput screening, with a large window that is stable over several hours. We note that the observed IC_{50} of cold ProTx-II peptide in the SPA assay is approximately 5-fold greater than that observed in filter binding experiments. The final SPA conditions required 5 ng of chimeric channel to yield an acceptable assay which corresponds to a 27-fold molar excess of chimeric protein over the radioligand. The lower potency of cold ProTx-II in the SPA format may be the result of ligand depletion. The effect of ligand depletion on measured IC50s ligand depletion as has been documented for other SPA assays (Carter et al., 2007). Scintillation proximity assays for other ion channels have been based on membrane preparations rather than purified protein (Hui et al., 2005; Zhang et al., 2006). One caution common to any chimera approach is the need to test any hits identified from a screen for activity against the wild-type $Na_V1.7$ in a functional assay.

Surface plasmon resonance (SPR) is a powerful method to study protein-peptide interactions in detail. Alpha-scorpion toxin binding to isolated $Na_V1.2$ VSD4 can be detected by SPR (Martin-Eauclaire et al., 2015). Here we show that an SPR assay based immobilization of an entire chimeric channel (DII S1-S4) is sensitive to ProTx-II binding. No binding was detectable with immobilized wild-type Na_VAb or the DII S3-S4 chimera, confirming that the SPR signal reflects a specific interaction with the $Na_V1.7$ DII chimera. Furthermore, the estimated K_d based on SPR aligns well with [^{125}I]ProTx-II binding competition and electrophysiology studies. A robust SPR assay for the DII S1-S4 chimera has several potential uses. For example, such an assay is ideal for confirming direct, specific interaction of novel molecules identified by screening with the chimera. Also, monoclonal antibodies identified from either traditional hybridoma approaches or phage panning can be tested for binding. Another obvious use of such an assay is the

Molecular Pharmacology Fast Forward. Published on June 23, 2017 as DOI: 10.1124/mol.117.108712
This article has not been copyedited and formatted. The final version may differ from this version.

biophysical characterization of the interaction of molecules with the chimeric channel, including kinetic and affinity estimates.

In summary, here we report a functional $Na_V1.7$ DII chimera with the bacterial channel Na_VAb. The chimera forms functional channels and is sensitive to the $Na_V1.7$ gating modifier peptide, ProTx-II. We demonstrate the utility of this chimera by engineering both SPA and SPR assays with purified protein. The DII S1-S4 chimera will prove useful for the discovery and characterization of novel molecules targeting this important functional domain of $Na_V1.7$. Furthermore, this chimera approach may have broad applicability for enabling screening at other membrane protein targets of pharmaceutical interest.

Molecular Pharmacology Fast Forward. Published on June 23, 2017 as DOI: 10.1124/mol.117.108712
This article has not been copyedited and formatted. The final version may differ from this version.

Authorship Contributions

Participated in research design: Ramkumar Rajamani, Mian Gao, John Watson, David R. Langley, Michael K. Ahlijanian, Linda J. Bristow, James Herrington

Conducted experiments: Sophie Wu , Iyoncy Rodrigo, Simon Low, Lisa Megson, David Wensel, Rick L. Pieschl, Debra J. Post-Munson, John Watson, James Herrington

Contributed new reagents or analytic tools: Mian Gao, Lisa Megson

Performed data analysis: Iyoncy Rodrigo, Simon Low, Lisa Megson, David Wensel, Rick L. Pieschl, Debra J. Post-Munson, John Watson, James Herrington

Wrote or contributed to the writing of the manuscript: Ramkumar Rajamani, Sophie Wu , Mian Gao, David Wensel, Rick L. Pieschl, John Watson, Michael K. Ahlijanian, Linda J. Bristow, James Herrington

Molecular Pharmacology Fast Forward. Published on June 23, 2017 as DOI: 10.1124/mol.117.108712
This article has not been copyedited and formatted. The final version may differ from this version.

References

Ahuja S, Mukund S, Deng L, Khakh K, Chang E, Ho H, Shriver S, Young C, Lin S, Johnson JP, Jr., Wu P, Li J, Coons M, Tam C, Brillantes B, Sampang H, Mortara K, Bowman KK, Clark KR, Estevez A, Xie Z, Verschoof H, Grimwood M, Dehnhardt C, Andrez JC, Focken T, Sutherlin DP, Safina BS, Starovasnik MA, Ortwine DF, Franke Y, Cohen CJ, Hackos DH, Koth CM and Payandeh J (2015) Structural basis of Nav1.7 inhibition by an isoform-selective small-molecule antagonist. *Science* **350**(6267): aac5464.

Alabi AA, Bahamonde MI, Jung HJ, Kim JI and Swartz KJ (2007) Portability of paddle motif function and pharmacology in voltage sensors. *Nature* **450**(7168): 370-375.

Bagneris C, DeCaen PG, Naylor CE, Pryde DC, Nobeli I, Clapham DE and Wallace BA (2014) Prokaryotic NavMs channel as a structural and functional model for eukaryotic sodium channel antagonism. *Proc Natl Acad Sci U S A* **111**(23): 8428-8433.

Bosmans F, Martin-Eauclaire MF and Swartz KJ (2008) Deconstructing voltage sensor function and pharmacology in sodium channels. *Nature* **456**(7219): 202-208.

Cao L, McDonnell A, Nitzsche A, Alexandrou A, Saintot PP, Loucif AJ, Brown AR, Young G, Mis M, Randall A, Waxman SG, Stanley P, Kirby S, Tarabar S, Gutteridge A, Butt R, McKernan RM, Whiting P, Ali Z, Bilsland J and Stevens EB (2016) Pharmacological reversal of a pain phenotype in iPSC-derived sensory neurons and patients with inherited erythromelalgia. *Sci Transl Med* **8**(335): 335ra356.

Carter CM, Leighton-Davies JR and Charlton SJ (2007) Miniaturized receptor binding assays: complications arising from ligand depletion. *J Biomol Screen* **12**(2): 255-266.

Catterall WA (2012) Voltage-gated sodium channels at 60: structure, function and pathophysiology. *J Physiol* **590**(11): 2577-2589.

Cox JJ, Reimann F, Nicholas AK, Thornton G, Roberts E, Springell K, Karbani G, Jafri H, Mannan J, Raashid Y, Al-Gazali L, Hamamy H, Valente EM, Gorman S, Williams R, McHale DP, Wood JN, Gribble FM and Woods CG (2006) An SCN9A channelopathy causes congenital inability to experience pain. *Nature* **444**(7121): 894-898.

Cox JJ, Sheynin J, Shorer Z, Reimann F, Nicholas AK, Zubovic L, Baralle M, Wraige E, Manor E, Levy J, Woods CG and Parvari R (2010) Congenital insensitivity to pain: novel SCN9A missense and in-frame deletion mutations. *Hum Mutat* **31**(9): E1670-1686.

Dib-Hajj SD, Cummins TR, Black JA and Waxman SG (2010) Sodium channels in normal and pathological pain. *Annu Rev Neurosci* **33**: 325-347.

Dib-Hajj SD, Yang Y, Black JA and Waxman SG (2013) The Na(V)1.7 sodium channel: from molecule to man. *Nat Rev Neurosci* **14**(1): 49-62.

Focken T, Liu S, Chahal N, Dauphinais M, Grimwood ME, Chowdhury S, Hemeon I, Bichler P, Bogucki D, Waldbrook M, Bankar G, Sojo LE, Young C, Lin S, Shuart N, Kwan R, Pang J, Chang JH, Safina BS, Sutherlin DP, Johnson JP, Jr., Dehnhardt CM, Mansour TS, Oballa RM, Cohen CJ and Robinette CL (2016) Discovery of Aryl Sulfonamides as Isoform-Selective Inhibitors of NaV1.7 with Efficacy in Rodent Pain Models. *ACS Med Chem Lett* **7**(3): 277-282.

Gamal El-Din TM, Martinez GQ, Payandeh J, Scheuer T and Catterall WA (2013) A gating charge interaction required for late slow inactivation of the bacterial sodium channel NavAb. *J Gen Physiol* **142**(3): 181-190.

Gingras J, Smith S, Matson DJ, Johnson D, Nye K, Couture L, Feric E, Yin R, Moyer BD, Peterson ML, Rottman JB, Beiler RJ, Malmberg AB and McDonough SI (2014) Global Nav1.7 knockout mice recapitulate the phenotype of human congenital indifference to pain. *PLoS One* **9**(9): e105895.

Goldberg YP, MacFarlane J, MacDonald ML, Thompson J, Dube MP, Mattice M, Fraser R, Young C, Hossain S, Pape T, Payne B, Radomski C, Donaldson G, Ives E, Cox J, Younghusband HB, Green R, Duff A, Boltshauser E, Grinspan GA, Dimon JH, Sibley BG, Andria G, Toscano E, Kerdraon J, Bowsher D, Pimstone SN, Samuels ME, Sherrington R and Hayden MR (2007) Loss-of-function

mutations in the Nav1.7 gene underlie congenital indifference to pain in multiple human populations. *Clin Genet* **71**(4): 311-319.

Henriques ST, Deplazes E, Lawrence N, Cheneval O, Chaousis S, Inserra M, Thongyoo P, King GF, Mark AE, Vetter I, Craik DJ and Schroeder CI (2016) Interaction of Tarantula Venom Peptide ProTx-II with Lipid Membranes Is a Prerequisite for Its Inhibition of Human Voltage-gated Sodium Channel NaV1.7. *J Biol Chem* **291**(33): 17049-17065.

Hui X, Gao J, Xie X, Suto N, Ogiku T and Wang MW (2005) A robust homogeneous binding assay for alpha4beta2 nicotinic acetylcholine receptor. *Acta Pharmacol Sin* **26**(10): 1175-1180.

Jones HM, Butt RP, Webster RW, Gurrell I, Dzygiel P, Flanagan N, Fraier D, Hay T, Iavarone LE, Luckwell J, Pearce H, Phipps A, Segelbacher J, Speed B and Beaumont K (2016) Clinical Micro-Dose Studies to Explore the Human Pharmacokinetics of Four Selective Inhibitors of Human Nav1.7 Voltage-Dependent Sodium Channels. *Clin Pharmacokinet* **55**(7): 875-887.

Klint JK, Smith JJ, Vetter I, Rupasinghe DB, Er SY, Senff S, Herzig V, Mobli M, Lewis RJ, Bosmans F and King GF (2015) Seven novel modulators of the analgesic target NaV 1.7 uncovered using a high-throughput venom-based discovery approach. *Br J Pharmacol* **172**(10): 2445-2458.

Lee JH, Park CK, Chen G, Han Q, Xie RG, Liu T, Ji RR and Lee SY (2014) A monoclonal antibody that targets a NaV1.7 channel voltage sensor for pain and itch relief. *Cell* **157**(6): 1393-1404.

Lee SY and MacKinnon R (2004) A membrane-access mechanism of ion channel inhibition by voltage sensor toxins from spider venom. *Nature* **430**(6996): 232-235.

Marheineke K, Grunewald S, Christie W and Reilander H (1998) Lipid composition of Spodoptera frugiperda (Sf9) and Trichoplusia ni (Tn) insect cells used for baculovirus infection. *FEBS Lett* **441**(1): 49-52.

Martin-Eauclaire MF, Ferracci G, Bosmans F and Bougis PE (2015) A surface plasmon resonance approach to monitor toxin interactions with an isolated voltage-gated sodium channel paddle motif. *J Gen Physiol* **145**(2): 155-162.

McCormack K, Santos S, Chapman ML, Krafte DS, Marron BE, West CW, Krambis MJ, Antonio BM, Zellmer SG, Printzenhoff D, Padilla KM, Lin Z, Wagoner PK, Swain NA, Stupple PA, de Groot M, Butt RP and Castle NA (2013) Voltage sensor interaction site for selective small molecule inhibitors of voltage-gated sodium channels. *Proc Natl Acad Sci U S A* **110**(29): E2724-2732.

Mihailescu M, Krepkiy D, Milescu M, Gawrisch K, Swartz KJ and White S (2014) Structural interactions of a voltage sensor toxin with lipid membranes. *Proc Natl Acad Sci U S A* **111**(50): E5463-5470.

Milescu M, Bosmans F, Lee S, Alabi AA, Kim JI and Swartz KJ (2009) Interactions between lipids and voltage sensor paddles detected with tarantula toxins. *Nat Struct Mol Biol* **16**(10): 1080-1085.

Milescu M, Vobecky J, Roh SH, Kim SH, Jung HJ, Kim JI and Swartz KJ (2007) Tarantula toxins interact with voltage sensors within lipid membranes. *J Gen Physiol* **130**(5): 497-511.

Minett MS, Falk S, Santana-Varela S, Bogdanov YD, Nassar MA, Heegaard AM and Wood JN (2014) Pain without nociceptors? Nav1.7-independent pain mechanisms. *Cell Rep* **6**(2): 301-312.

Minett MS, Nassar MA, Clark AK, Passmore G, Dickenson AH, Wang F, Malcangio M and Wood JN (2012) Distinct Nav1.7-dependent pain sensations require different sets of sensory and sympathetic neurons. *Nat Commun* **3**: 791.

Murray JK, Biswas K, Holder JR, Zou A, Ligutti J, Liu D, Poppe L, Andrews KL, Lin FF, Meng SY, Moyer BD, McDonough SI and Miranda LP (2015a) Sustained inhibition of the NaV1.7 sodium channel by engineered dimers of the domain II binding peptide GpTx-1. *Bioorg Med Chem Lett* **25**(21): 4866-4871.

Murray JK, Ligutti J, Liu D, Zou A, Poppe L, Li H, Andrews KL, Moyer BD, McDonough SI, Favreau P, Stocklin R and Miranda LP (2015b) Engineering potent and selective analogues of GpTx-1, a tarantula venom peptide antagonist of the Na(V)1.7 sodium channel. *J Med Chem* **58**(5): 2299-2314.

Molecular Pharmacology Fast Forward. Published on June 23, 2017 as DOI: 10.1124/mol.117.108712
This article has not been copyedited and formatted. The final version may differ from this version.

Murray JK, Long J, Zou A, Ligutti J, Andrews KL, Poppe L, Biswas K, Moyer BD, McDonough SI and Miranda LP (2016) Single Residue Substitutions That Confer Voltage-Gated Sodium Ion Channel Subtype Selectivity in the NaV1.7 Inhibitory Peptide GpTx-1. *J Med Chem* **59**(6): 2704-2717.

Park JH, Carlin KP, Wu G, Ilyin VI, Musza LL, Blake PR and Kyle DJ (2014) Studies examining the relationship between the chemical structure of protoxin II and its activity on voltage gated sodium channels. *J Med Chem* **57**(15): 6623-6631.

Payandeh J, Gamal El-Din TM, Scheuer T, Zheng N and Catterall WA (2012) Crystal structure of a voltage-gated sodium channel in two potentially inactivated states. *Nature* **486**(7401): 135-139.

Payandeh J, Scheuer T, Zheng N and Catterall WA (2011) The crystal structure of a voltage-gated sodium channel. *Nature* **475**(7356): 353-358.

Schmalhofer WA, Calhoun J, Burrows R, Bailey T, Kohler MG, Weinglass AB, Kaczorowski GJ, Garcia ML, Koltzenburg M and Priest BT (2008) ProTx-II, a selective inhibitor of NaV1.7 sodium channels, blocks action potential propagation in nociceptors. *Mol Pharmacol* **74**(5): 1476-1484.

Shen H, Zhou Q, Pan X, Li Z, Wu J and Yan N (2017) Structure of a eukaryotic voltage-gated sodium channel at near-atomic resolution. *Science* **355**(6328).

Smith JJ, Alphy S, Seibert AL and Blumenthal KM (2005) Differential phospholipid binding by site 3 and site 4 toxins. Implications for structural variability between voltage-sensitive sodium channel domains. *J Biol Chem* **280**(12): 11127-11133.

Smith JJ, Cummins TR, Alphy S and Blumenthal KM (2007) Molecular interactions of the gating modifier toxin ProTx-II with NaV 1.5: implied existence of a novel toxin binding site coupled to activation. *J Biol Chem* **282**(17): 12687-12697.

Sokolov S, Kraus RL, Scheuer T and Catterall WA (2008) Inhibition of sodium channel gating by trapping the domain II voltage sensor with protoxin II. *Mol Pharmacol* **73**(3): 1020-1028.

Thomas-Tran R and Du Bois J (2016) Mutant cycle analysis with modified saxitoxins reveals specific interactions critical to attaining high-affinity inhibition of hNaV1.7. *Proc Natl Acad Sci U S A* **113**(21): 5856-5861.

Tilley DC, Eum KS, Fletcher-Taylor S, Austin DC, Dupre C, Patron LA, Garcia RL, Lam K, Yarov-Yarovoy V, Cohen BE and Sack JT (2014) Chemoselective tarantula toxins report voltage activation of wild-type ion channels in live cells. *Proc Natl Acad Sci U S A* **111**(44): E4789-4796.

Walker JR, Novick PA, Parsons WH, McGregor M, Zablocki J, Pande VS and Du Bois J (2012) Marked difference in saxitoxin and tetrodotoxin affinity for the human nociceptive voltage-gated sodium channel (Nav1.7) [corrected]. *Proc Natl Acad Sci U S A* **109**(44): 18102-18107.

Wilson MJ, Zhang MM, Azam L, Olivera BM, Bulaj G and Yoshikami D (2011) Navbeta subunits modulate the inhibition of Nav1.8 by the analgesic gating modifier muO-conotoxin MrVIB. *J Pharmacol Exp Ther* **338**(2): 687-693.

Wu J, Yan Z, Li Z, Qian X, Lu S, Dong M, Zhou Q and Yan N (2016) Structure of the voltage-gated calcium channel Cav1.1 at 3.6 A resolution. *Nature* **537**(7619): 191-196.

Wu J, Yan Z, Li Z, Yan C, Lu S, Dong M and Yan N (2015) Structure of the voltage-gated calcium channel Cav1.1 complex. *Science* **350**(6267): aad2395.

Xiao Y, Blumenthal K and Cummins TR (2014) Gating-pore currents demonstrate selective and specific modulation of individual sodium channel voltage-sensors by biological toxins. *Mol Pharmacol* **86**(2): 159-167.

Xiao Y, Blumenthal K, Jackson JO, 2nd, Liang S and Cummins TR (2010) The tarantula toxins ProTx-II and huwentoxin-IV differentially interact with human Nav1.7 voltage sensors to inhibit channel activation and inactivation. *Mol Pharmacol* **78**(6): 1124-1134.

Zhang JH, Chung TD and Oldenburg KR (1999) A Simple Statistical Parameter for Use in Evaluation and Validation of High Throughput Screening Assays. *J Biomol Screen* **4**(2): 67-73.

Zhang SP, Kauffman J, Yagel SK and Codd EE (2006) High-throughput screening for N-type calcium channel blockers using a scintillation proximity assay. *J Biomol Screen* **11**(6): 672-677.

Zhang X, Ren W, DeCaen P, Yan C, Tao X, Tang L, Wang J, Hasegawa K, Kumasaka T, He J, Wang J, Clapham DE and Yan N (2012) Crystal structure of an orthologue of the NaChBac voltage-gated sodium channel. *Nature* **486**(7401): 130-134.

Molecular Pharmacology Fast Forward. Published on June 23, 2017 as DOI: 10.1124/mol.117.108712
This article has not been copyedited and formatted. The final version may differ from this version.

Figure Legends

Figure 1. Design of Na$_V$1.7- Na$_V$Ab chimeras. Sequence alignment of the S1-S2 (top) and S3-S4 (bottom) regions of human Na$_V$1.7 domains DII with Na$_V$Ab. The splice junctions chosen for creation of chimeras are designated by the anchor symbols.

Figure 2. [^{125}I]ProTx-II binding of Na$_V$1.7- Na$_V$Ab chimeras. A. [^{125}I]ProTx-II binding to h Na$_V$1.7 channels expressed in HEK293 cells. For whole-cell binding (left), 15,000 cells per well in a 96-well plate were incubated with 0.36 nM [^{125}I]-ProTx-II. Non-specific (NS) binding was defined by addition of 0.6 μM cold ProTx-II. Bars represent the mean ± SEM cpms, n=6. For membranes (right), 50 μg h Na$_V$1.7 HEK membranes were incubated with 0.15 nM [^{125}I]-ProTx-II. Non-specific binding was defined by addition of 1 μM cold ProTx-II. Bars represent the mean ± SEM cpms, n=3. B. 1 μg Sf9 membranes from non-transduced cells (Sf9) or cells transduced with either wt Na$_V$Ab, DII S3-S4 chimera or DII S1-4 chimera were incubated with 1.2 nM [^{125}I]-ProTx-II. Non-specific binding was defined by addition of 20 μM cold ProTx-II. Bars represent the mean ± SEM cpms, n=3. C. Purified DII S1-S4 protein (0.003-3.0 μg) was incubated with 1.9 nM [^{125}I]-ProTx-II. Non-specific binding was defined by addition of 0.6 μM cold ProTx-II. Bars represent the mean ± SEM cpms, n=3. D. Percent inhibition of specific [^{125}I]-ProTx-II (1.1 nM) binding to purified DII S1-S4 protein (0.3 μg) by cold ProTx-II (circles) and Huwentoxin-IV (squares). Non-specific binding was defined by addition of 2 μM cold ProTx-II. Symbols represent the mean ± SEM inhibition of three independent experiments measured in triplicate. Estimated IC50s from the fits are 36 nM (ProTx-II) and 662 nM (Huwentoxin-IV).

Molecular Pharmacology Fast Forward. Published on June 23, 2017 as DOI: 10.1124/mol.117.108712
This article has not been copyedited and formatted. The final version may differ from this version.

Figure 3. DII S1-S4 chimera forms functional, ProTx-II sensitive channels. A. Representative recording from a Sf9 cell transduced with BacMam encoding DII S1-S4 chimera. Currents were evoked by 20 msec step depolarizations between -140 mV and +120 mV. For clarity, only step depolarizations between -20 mV and +100 mV in 20 mV increments are shown. B. Plot of the mean ± SEM relative conductance of Na_VAb (circles, n=9), h $Na_V1.7$ (diamonds, n=12) and DII S1-S4 chimera (squares, n=9) versus membrane potential. The solid lines are fits of the Boltzmann equation to the data. Parameters of the fits are given in Table 1. C. Representative recording from a Sf9 cell transduced with BacMam encoding DII S1-S4 chimera. Currents were evoked by a 20 msec step depolarization to +60 mV in control and in the presence of 10 nM ProTx-II. D. Plot of the relative conductance versus membrane potential for the recording in panel C in control (circles) and 100 nM ProTx-II (triangles). Conductance was estimated from the tail current amplitude and normalized to the control amplitude at the +120 mV test potential.

Figure 4. Surface plasmon resonance (SPR) binding assay for DII S1-S4 chimera. A and B. Biacore T200 SPR sensorgrams showing binding profiles of his-tagged ProTx-II (A; 100 nM) or Huwentoxin-IV (B; 1000 nM) to biotinylated Na_VAb (black), DII S3-S4 (blue) or DII S1-S4 (red). C. Binding of a duplicate 2-fold concentration series (7.8 nM to 1000 nM) of ProTx-II to DII S1-S4. Each color indicates a separate concentration in the series. D. Binding of a duplicate 2-fold concentration series (7.8 nM to 1000 nM) of Huwentoxin-IV (62.5 nM to 1000 nM) to DII S1-S4. Each color indicates a separate concentration in the series. Blank buffer injections as well as background binding to a Neutravidin-only flow cell have been subtracted from all displayed sensorgrams.

Molecular Pharmacology Fast Forward. Published on June 23, 2017 as DOI: 10.1124/mol.117.108712
This article has not been copyedited and formatted. The final version may differ from this version.

Figure 5. Scintillation proximity assay (SPA) with DII S1-S4 chimera in 1536-well format. A. Competition of the SPA luminescence signal (relative light units, RLU) by cold ProTx-II after a 4 h incubation. Symbols are the mean ± SD of four replicate wells. The solid line is a 4-parameter fit with an IC_{50} of 107 nM and Hill slope of 0.95. B. Plot of the pIC_{50} of competition by cold ProTx-II versus time. C. Plot of the signal-to-background ratio versus time. D. Plot of the assay Z' statistic versus time. The signal-to-background ratio and Z' statistic were calculated using 2 columns each (32 wells) for the assay high and low signals.

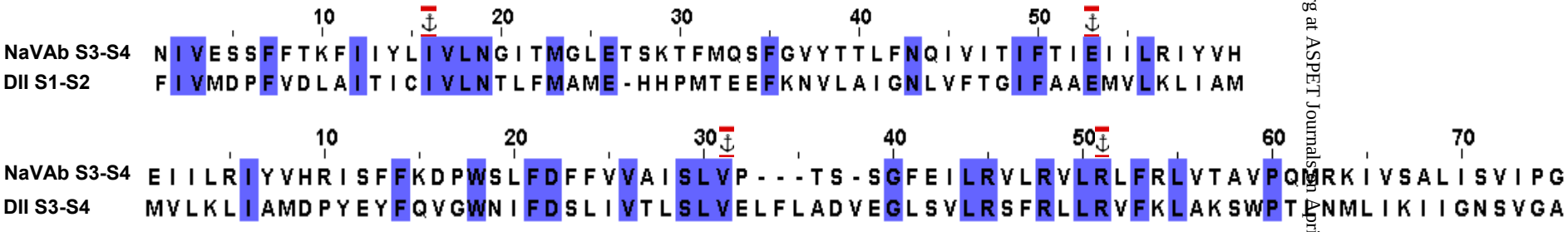

Figure 1

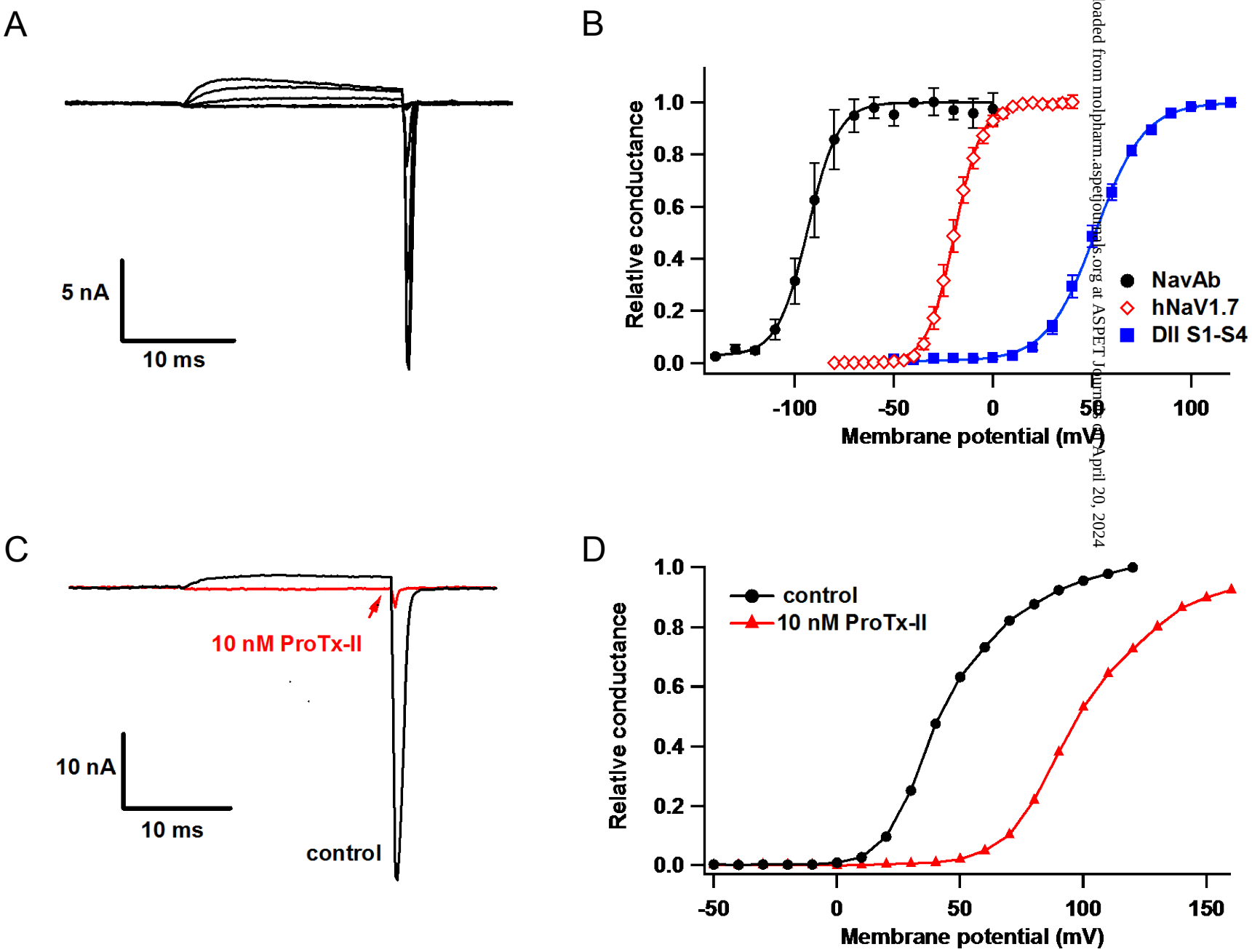

Figure 2

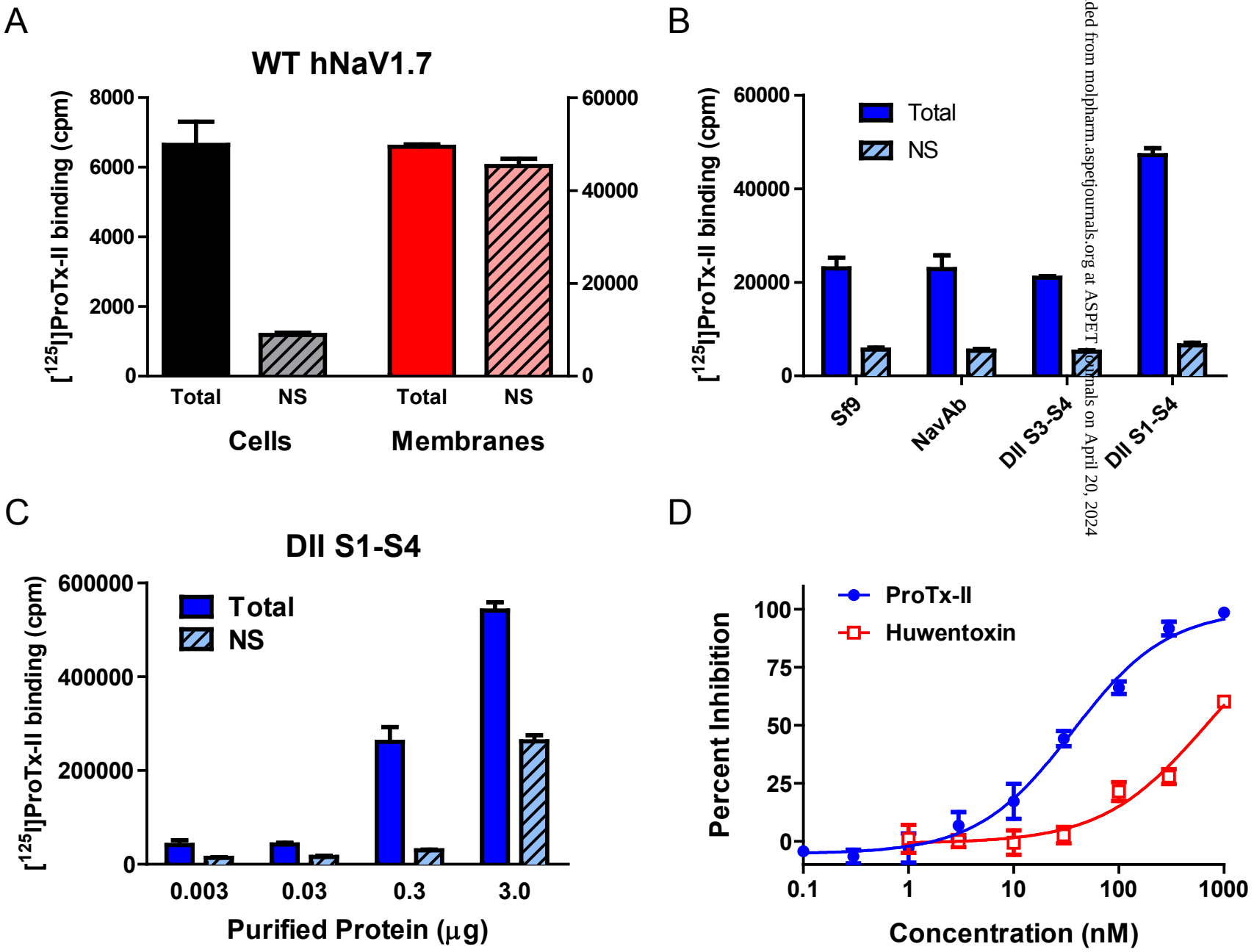

Figure 3

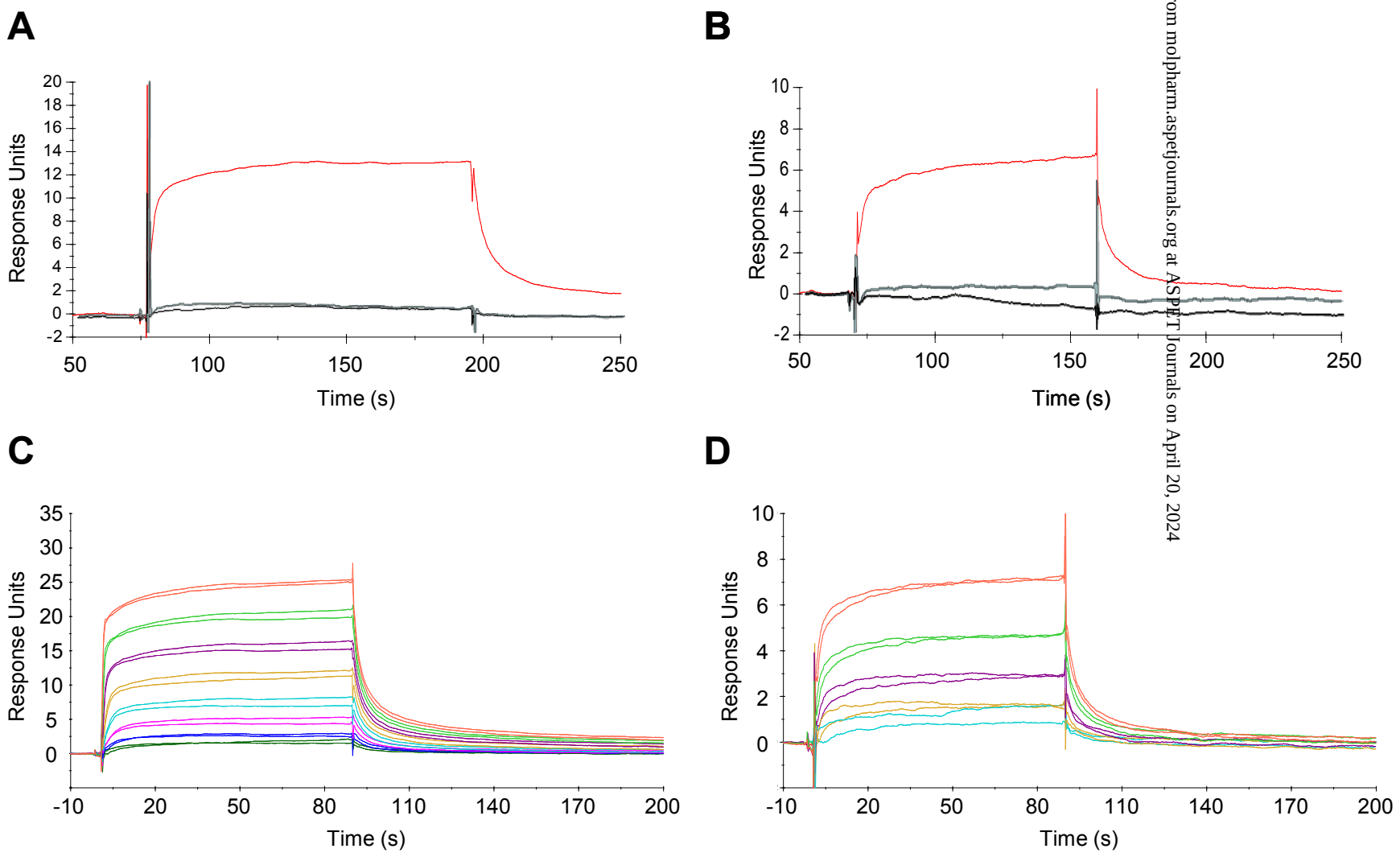

Figure 4

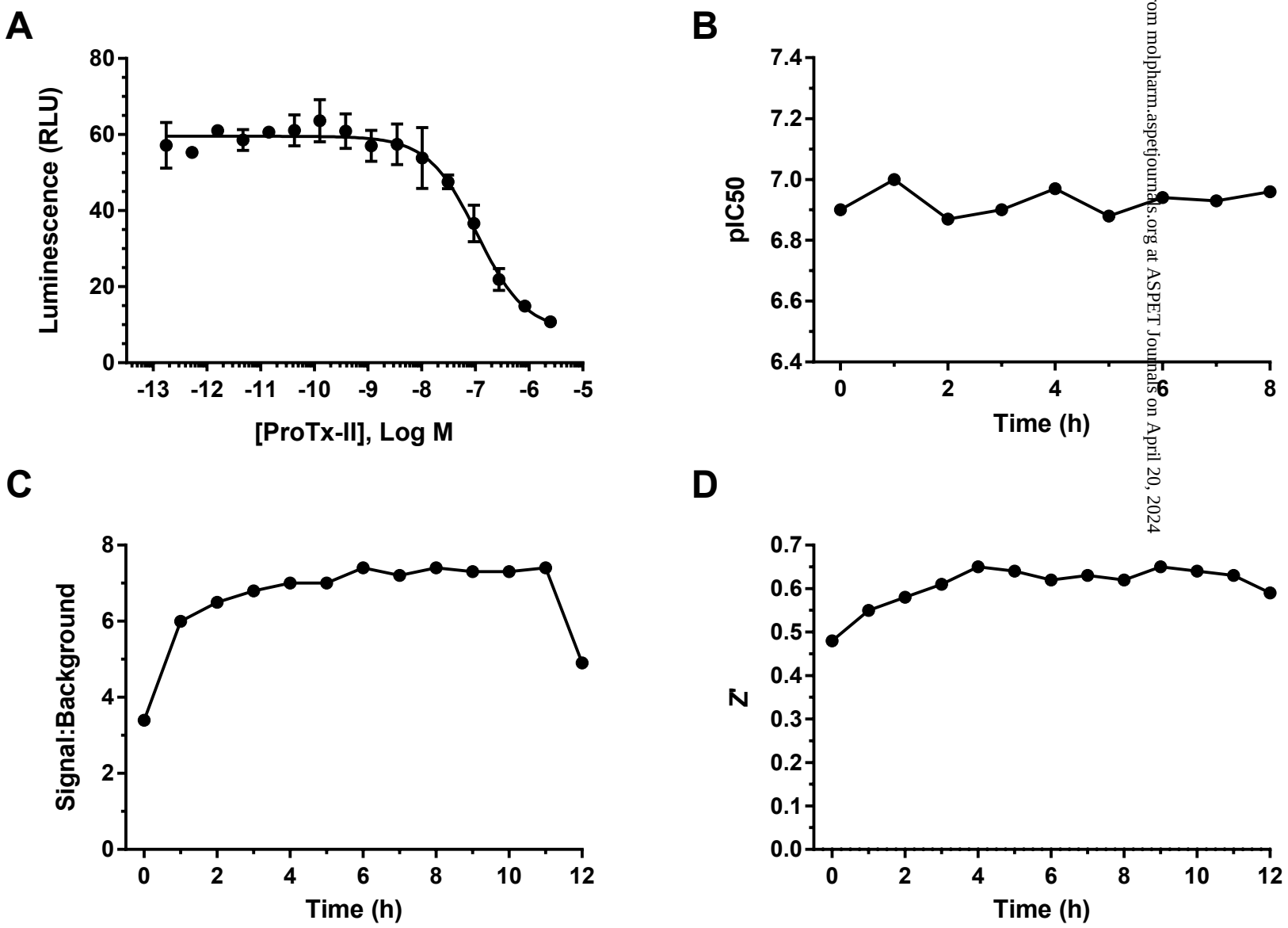

Figure 5